The Pharma Innovation Journal 2019; 8(2): 407-413

www.ThePharmaJournal.com

The Pharma Innovation

ISSN (E): 2277- 7695
ISSN (P): 2349-8242
NAAS Rating: 5.03
TPI 2019; 8(2): 407-413

www.thepharmajournal.com
Received: 09-12-2018
Accepted: 13-01-2019

Guguloth Ramesh
Department of Veterinary Pathology, P.V.N.R.T.V.U, Hyderabad, Telangana, India

D Madhuri
Department of Veterinary Pathology, P.V.N.R.T.V.U, Hyderabad, Telangana, India

M Lakshman
Department of Veterinary Pathology, P.V.N.R.T.V.U, Hyderabad, Telangana, India

Alla Gopal Reddy
Department of Veterinary Pharmacology and Toxicology, P.V.N.R.T.V.U, Hyderabad, Telangana, India

Correspondence
Guguloth Ramesh
Department of Veterinary Pathology, P.V.N.R.T.V.U, Hyderabad, Telangana, India

Histopathological and ultrastructural changes of liver and kidney induced by lead and cadmium alone and combined exposure in male wistar rats

Guguloth Ramesh, D Madhuri, M Lakshman and Alla Gopal Reddy

Abstract
In the present study renal and hepatic toxicity was assessed by histopathological and ultrastructural evaluation of liver and kidney tissues of rats exposed to lead and cadmium alone and in combination. Forty eight male albino Wistar rats were divided into 4 groups 12 rats in each group; group 1(control) was given deionized water, group 2 (lead group) was given water with lead acetate @ 30 mg/kg b.wt, group 3 (cadmium group) was given water with cadmium chloride @15 mg/kg b.wt, and group 4 (combined group) was given water with both lead acetate@ 30 mg/kg b.wt and cadmium chloride @15 mg/kg b.wt for 28 days. The histopathological changes in liver revealed congestion, sinusoidal dilatation, vacuolar degeneration, infiltration of MNCs in hepatic parenchyma and bile duct hyperplasia. Kidney sections showed degenerative changes in tubules, congestion, inter tubular hemorrhages and presence of casts. Scanning electron microscopy of liver revealed abnormal erythrocytes and accumulation of lead and cadmium in the tissues.
Transmission electron microscopy of liver of group 2, group 3 and group 4 revealed swollen to condensed and pyknotic nucleus, electron dense material in nucleus, mitochondrial changes like swollen to condensed mitochondria, increased number of mitochondria and ruptured endoplasmic reticulum. Kidney showed swollen nucleus with condensed nucleolus and margination of chromatin, cytoplasm showed vacuolation, swollen mitochondria with electron dense material, epithelium of tubules showed dilation of nuclear pore along with margination of chromatin.

Keywords: cadmium, histopathology, lead, rats, toxicity, ultrastructural changes

Introduction
Environmental pollution is a global problem for man and animals. Pollutants from industrial waste enter into the livestock production systems and then into food chain. Lead and cadmium are the two most abundant toxic metals in the environment. The common sources of lead and cadmium are diverse in nature including natural and anthropogenic processes such as combustion of coal and mineral oil, smelters, mining and alloy processing units and paint industries. Constantly increasing environmental pollutants due to increased urbanization, industrialization and through the scientific and technical advances have stimulated interest in the study of toxic substances and its consequences to biological system [18]. Lead toxicity is largely due to its capacity to mimic calcium and substitute it in many of the fundamental cellular processes that depends on calcium. Thus the highest concentration of lead are usually found in bone, liver and kidneys [9]. Cd toxicity promotes the induction of various pathological events via free radical initiation mechanism which produces active oxidative free radicals from biological components of cells such as lipids, proteins and DNA.

Material and Methods
Chemicals
Lead acetate and cadmium chloride were procured from Thermo Fisher Scientific India. Pvt. Ltd. Mumbai.

Experimental animals
Adult male albino rats (*Wistar* strain*)* weighing 250-280g and 6 weeks of age, were procured from Sanzyme laboratories Ltd., Hyderabad. The experiment was carried out according to the guidelines and prior approval of the Institutional Animal Ethics Committee (IAEC) (No.18-2017 SA).

Experimental design

A total of 48 male albino Wistar rats were randomly divided into 4 groups consisting of 12 in each group. Group 1(control) was given deionized water, group 2(lead group) was given water with lead acetate @30 mg/kg b.wt, group 3(cadmium group) was given water with cadmium chloride @15 mg/kg b.wt and group 4 (combined group) was given water with both lead acetate @ 30 mg/kg b.wt and cadmium chloride @15 mg/kg b.wt for 28 days respectively.

Methods

To study the gross and histopathology, six rats from each group were sacrificed on 14th and 28th day of experimental period. Detailed necropsy was conducted and gross changes if any recorded. Pieces of liver and kidney were collected in fixative neutral buffered formalin (NBF) for histopathology. Samples were processed, sectioned (5µm), stained with Hematoxylin and Eosin (H&E) as per the standard protocol [14].

For electron microscopic study, tissue samples of liver and kidney were fixed in 2.5% (percent) gluteraldehyde (PBS based EM grade) and processed as per the standard protocol [4].

Results

Grossly liver of Group 1 rats showed normal appearance where as liver of Group 2 and Group 4 rats on 14th day showed mild hepatomegaly and congestion. In Group 3, on 14th day no appreciable gross lesions were observed. On 28th day, mild to moderate hepatomegaly in Group 2 and Group 3 and slightly pale and friable liver was noticed in Group 4.

Normal appearance of kidney was noticed in Group 1 rats whereas mild congestion was noticed in Group 2, Group 3 and Group 4 on 28th day of experimental period respectively.

Histopathological examination of liver section from control (Group 1) rats on 14th day and 28th day of experimental period showed normal hepatic parenchyma with central vein and portal triad.

The section of liver of Group 2 rats on 14th day showed dilated sinusoidal spaces along with congestion, mild infiltration of mononuclear cells (MNCs) in the hepatic parenchyma (Fig.1) and moderate vacuolar degeneration. On 28th day severe vacuolar degenerative changes, necrosis of hepatocytes with marked infiltration of MNCs was noticed (Fig 2). The section of liver on 14th day of experimental period of Cd intoxicated rats (Group 3) showed mild MNCs infiltration and vacuolar degeneration (Fig. 3). On 28th day, liver section revealed moderate dilatation of sinusoids, mild to moderate MNCs infiltration in hepatic parenchyma as well as in the portal triad and multifocal areas of coagulative necrosis. In Group 4 rats the liver section showed mild bile duct hyperplasia (Fig. 4), severe vacuolar degeneration (Fig. 5) and necrosis of hepatocytes with mild to moderate infiltration of MNCs at 14th day of the experiment and the above mentioned changes were severe on 28th day of the experiment (Fig. 6).

Section of kidney of Group 1 rats showed normal parenchyma of kidney. The kidney of Group 2 rats on 14th day showed mild to moderate vacuolar degeneration, desquamation of epithelial cells from basement membrane, mild to moderate congestion and inter tubular hemorrhages. On 28th day severe degenerative and necrotic changes in tubules was noticed (Fig. 7). The lesions in glomeruli were characterized by increased Bowmen's space, atrophy, vacuolation and hemorrhages in glomerulus tufts. Epithelial and hyaline casts were noticed in the lumen of tubules (Fig. 7).

Kidney sections of Group 3 rats on 14th day showed tubular degeneration, mononuclear cell infiltration in the interstitium, congestion and marked inter tubular hemorrhages. In addition glomeruli showed atrophy and increased glomerular space. On 28th day, mononuclear cell infiltration in the interstitium (Fig. 8) and presence of casts was seen in the lumen of tubules (Fig. 9). The intensity of lesions was more pronounced in Group 4 as compared to Group 3 (Fig.10).

Scanning electron microscopy of Group 2 and Group 3 rat liver showed abnormal RBC (folded, hat shaped) (Fig.11) and electron dense granular material deposition around the vein (Fig. 12 and 13) on 14th and 28th day of experiment.

Liver of Group 4 rats showed multiple deposition of electron dense granular material (lead and cadmium) on surface area (Fig.14) and complete loss of architectural details on 14th and 28th day of experiment.

TEM (Transmission electron microscopy) section of Group 2 rat liver showed dilated sinusoids, swollen to condensed and pyknotic nucleus and electron dense material in nucleus. Cytoplasm of these cells showed vacuolation, granular cytoplasm and electron dense material in cytosol. Mitochondrial changes like swollen to condensed mitochondria, increased number of mitochondria and ruptured rough endoplasmic reticulum (RER) (Fig.15) were observed. Group 3 showed loss of architecture of the hepatocytes, cytoplasmic vacuolation, electron dense material in mitochondria and thickened intercellular junction (Fig.16). In addition some sections showed eccentrically placed nucleus, collapsed nuclear membrane, pyknotic and rhexis of nuclei, clumping of condensed granular chromatin material and margination of chromatin (Fig.17). In Group 4 the above changes were more marked and severe (Fig.18).

The ultra structure of Group 2 kidney section revealed loss of architecture, severe dilation of intertubular area and loss of tubular epithelium topography. A few sections revealed swollen nucleus with condensed nucleolus and margination of chromatin and intact brush border. Cytoplasm showed vacuolation of tubular epithelium, severe dilatation of intertubular area and electron dense mitochondria of varied size and numerous round electron dense bodies in nucleus (Fig. 19). Group 3 kidney showed vacuolar degeneration and severe dilation of tubules, some tubules showed degeneration of epithelial cells with pyknotic nucleus and swollen mitochondria. Epithelium of tubules showed dilation of nuclear pore along with margination of chromatin materials (Fig. 20). Few other sections revealed disruption of nuclear membrane, pyknotic nuclei and electron dense round bodies in the nucleus (Fig. 21), retention of brush border and scanty cytoplasm along with mitochondria were observed. Kidney of Group 4 showed complete loss of architectural details though outlines of nucleus and mitochondria remained. Few other sections revealed vacuolated cytoplasm, narrow and tight inter tubular junction, thick nuclear membrane, increased perinuclear space, distorted mitochondria cistern arranged in rows around the nucleus, discontinuation of RER, vesiculated nucleus and dilation of nuclear pore (Fig. 22).

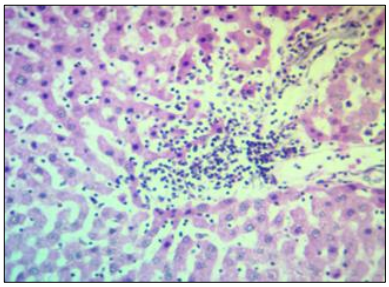

Fig 1: Microphotograph of Group 2 liver, showing sinusoidal dilatation and infiltration with MNC in parenchyma on 14th day. H&E×400.

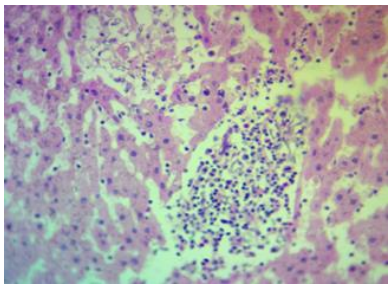

Fig 2: Microphotograph of Group 2 liver showing sinusoidal dilatation and infiltration with MNCs in parenchyma and necrosis on 28th day. H&E×400.

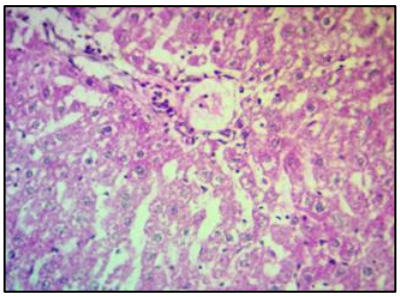

Fig 3: Microphotograph of Group 3 liver showing mild to moderate vacuolar degeneration and mild infiltration of MNCs on 14th day. H&E×400.

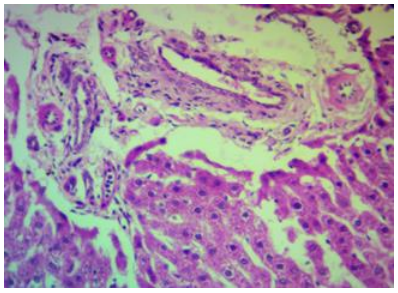

Fig 4: Microphotograph of Group 4 liver showing bile duct hyperplasia on 14th day. H&E×400.

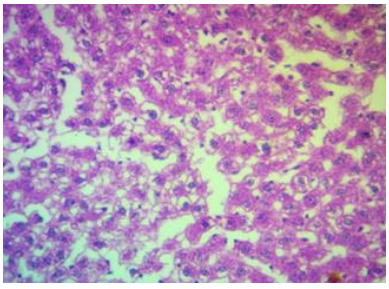

Fig 5: Microphotograph of Group 4 liver showing severe vacuolar degeneration on14th day. H&E×400

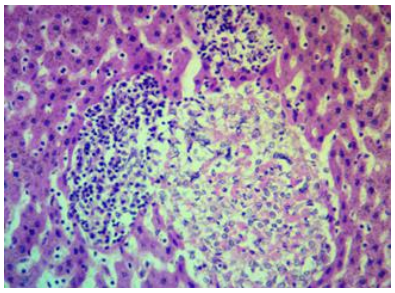

Fig 6: Microphotograph of Group 4 liver showing sinusoidal dilatation and aggregation of MNCs and necrosis of hepatocytes on 28th day. H&E×400.

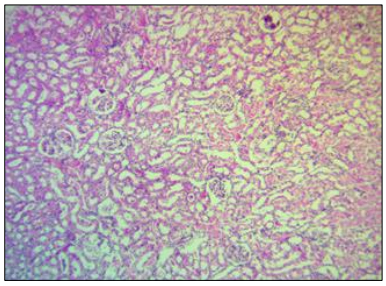

Fig 7: Microphotograph of Group 2 kidney showing marked inter tubular hemorrhages, degeneration of tubular epithelium, necrosis, cast in the tubules and glomerular atrophy on 28th day. H&E×100.

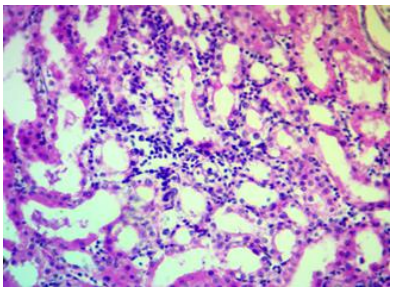

Fig 8: Microphotograph of Group 3 kidney showing severe interstitial aggregation of MNC on 28th day. H&E×400

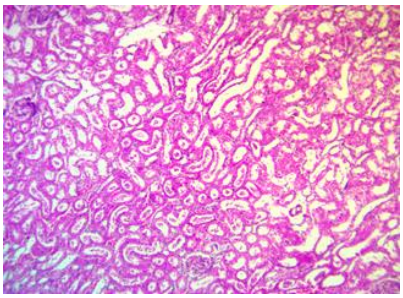

Fig 9: Microphotograph of Group 3 kidney showing presence of cast in most of the tubules on 28th day. H&E×100.

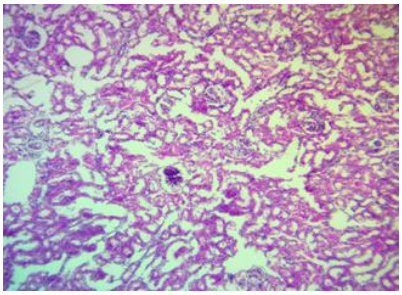

Fig 10: Microphotograph of Group 4 kidney showing atrophy of glomeruli, severe tubular degeneration and necrosis on 28th day. H&E×400

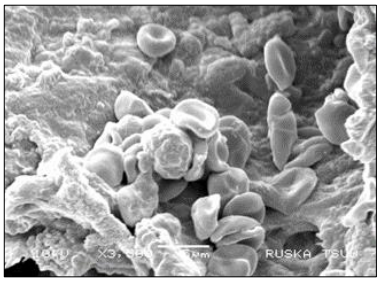

Fig 11: Scanning electron micrograph of Group 2 liver showing abnormal erythrocytes (folded, hat shaped) on 28th day.

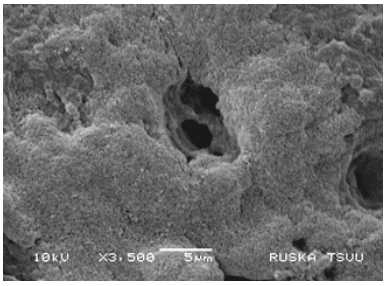

Fig 12: Scanning electron micrograph of Group 2 liver showing electron dense granular material deposition (lead) around vein on 28th day.

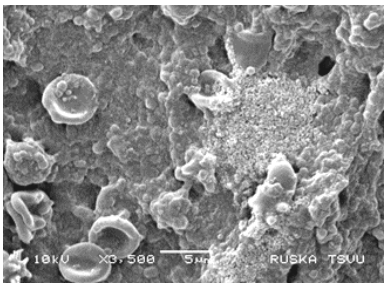

Fig 13: Scanning electron micrograph of Group 3 liver showing abnormal erythrocytes and electron dense granular material deposition (cadmium) on 28th day

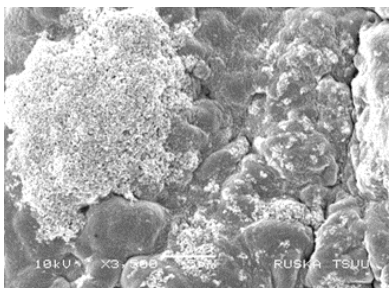

Fig 14: Scanning electron micrograph of Group 4 liver showing multiple electron dense granular material deposition (lead and cadmium) deposits of on 28th day.

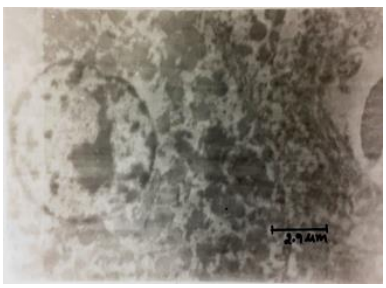

Fig 15: Transmission electron micrograph of hepatocyte showing clumping of RER, electron dense mitochondria and condensed chromatin. UA & LC 6755x (Group 2, day 28).

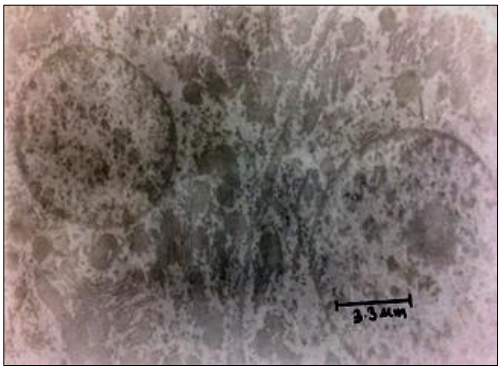

Fig 16: Transmission electron micrograph of hepatocytes showing thickened inter cellular junction, cytoplasmic vacuolation, electron dense material in cytosol, swollen and condensed nuclei and granular nucleoplasm. UA & LC 5790x (Group 3, day 28).

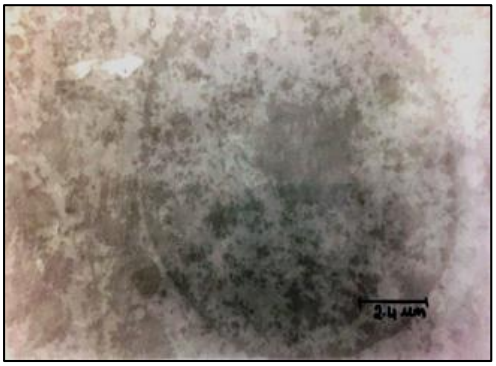

Fig 17: Transmission electron micrograph of hepatocyte showing mild granular material in nucleoplasm margination of chromatin material. UA & LC 9650x (Group 3, day 28).

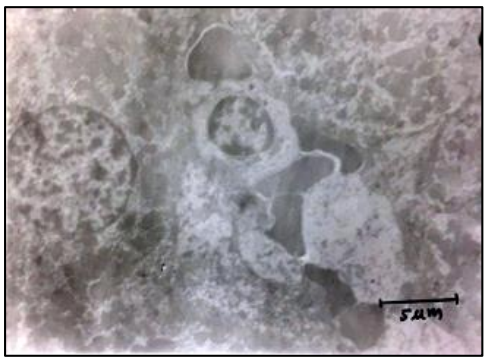

Fig 18: Transmission electron micrograph of hepatocyte showing loose cell junction, shrunken cell with condensed mitochondria and nuclei. UA & LC 3860x (Group 4, day 28).

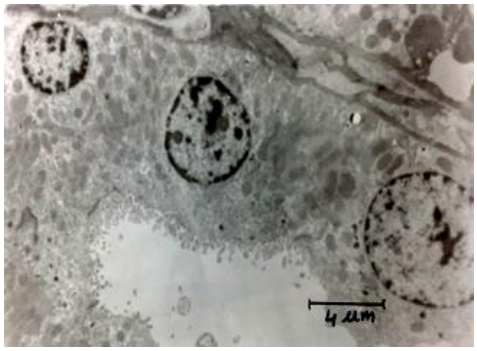

Fig 19: Transmission electron micrograph of kidney showing altered shape of mitochondria, swollen nucleus, condensed nucleolus and margination of chromatin material. UA & LC 4825x (Group 2, day 28).

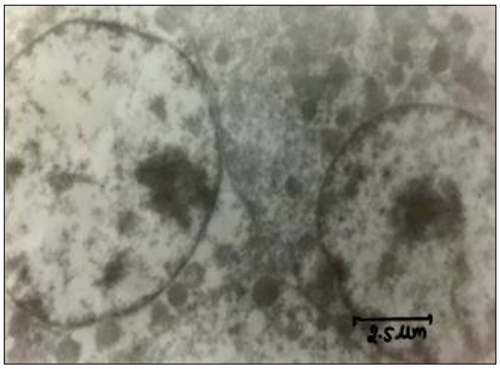

Fig 20: Transmission electron micrograph of kidney showing vacuolar degeneration of cytoplasm, electron dense mitochondria, swollen nucleus, condensed nucleolus and. UA & LC 4825x (Group 3, day 28).

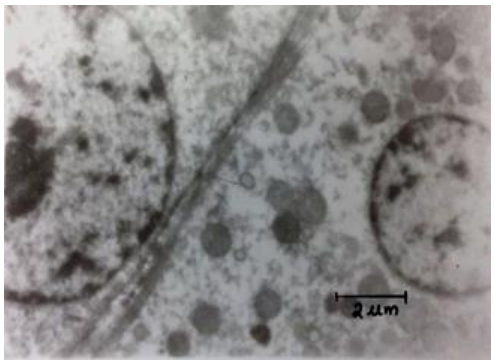

Fig 21: Transmission electron micrograph of kidney showing electron dense mitochondria of varied size and shape, swollen nuclei and condensed chromatin. UA & LC 9650x (Group 3, day 28).

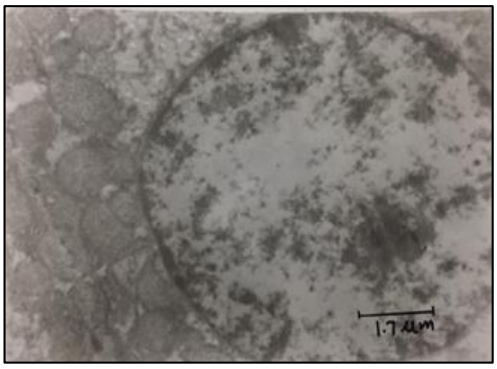

Fig 22: Transmission electron micrograph of kidney showing Vacuolated cytoplasm, electron dense mitochondria of varied size and shape, thick nuclear membrane, distorted Chromatin and severe margination of chromatin material. UA & LC 11580x (Group 4, day 28).

Discussion

In the present study toxic effects of lead, cadmium either alone or in combination on liver and kidneys was studied. In Group 2 mild to moderate enlargement of liver and congestion was noticed and these were in agreement with research workers [1, 26, 27]. These lesions might be attributed to the toxic effect and high production of free radicals which ultimately created stress on liver [8, 22].

Mild congestion of kidneys was noticed in Group 2, Group 3 and Group 4 on 14th and 28th day of experimental period. Similar changes were also noticed by [25, 26, 27]. The probable reason for the lesions noticed might be due to the toxic effect of lead and cadmium.

Histopathological examination of liver sections from Group 2 rats on 14th day showed mild congestion, mild infiltration of MNCs, sinusoidal dilatation and vacuolar degeneration, similar lesions were also noticed by Hegazy and Fouad [10, 27]. On 28th day marked vacuolar degenerative changes, necrosis of hepatocytes with marked periportal infiltration of MNCs was related to the findings of Jarrar and Taib [11, 15].

Group 3 rats on 14th day revealed mild leucocytic infiltration around portal triad, and increased Kupffer cells in sinusoids of hepatic parenchyma. On 28th day, intensity of MNC infiltration increased in the hepatic parenchyma and around portal triad. Moderate dilatation of sinusoids, focal areas of lymphoid aggregation, congested blood vessels, multifocal areas of coagulative necrosis, swelling of hepatocytes with vacuolar degeneration, these results were lined with [21].

Lesions in Group 4 rats were severe and progressive where lead and cadmium had potentiated effect on co exposure. Similarly few investigators also observed synergistic effect of lead and cadmium on testicular tissue [16, 17].

Histopathological examination of kidney sections from Group 2 rats revealed mild to moderate vacuolar degeneration, desquamation of epithelial cells from basement membrane, mild to moderate congestion, intertubular hemorrhages in medullary and cortical region and similar changes were documented by [2, 27]. On 28th day, severe degenerative and necrotic changes noticed which were prominent in tubules than the glomeruli. In Group 4 similar lesions were observed but were more severe in nature.

Group 3 rats, kidney revealed tubular degeneration, focal areas of necrosis, tubular dilatation, mononuclear cell infiltration in the interstitium, congestion, marked intertubular hemorrhages, desquamation of epithelial cells from basement membrane and casts in the lumen of tubules. The glomeruli showed atrophy, increased glomerular space vacuolar degeneration and mononuclear cell infiltration [28]. On 28th day lesions were progressive and severe. These changes might be due to the accumulation of free radicals as the consequence of increased lipid peroxidation by free Cd ions in the renal tissues of Cd-treated rats [23]. Another possible reason might be due to cytotoxic effects of Cd in the liver and kidney which promotes apoptotic cell production, formation of nuclear DNA fragmentation, and release of mitochondrial apoptotic proteins after exposure to $CdCl_2$ and were accompanied by ROS generation [12, 13].

SEM studies of Liver on 28th day showed loss of architectural details, abnormal erythrocytes and electron dense granular material deposition (lead) around vein in Group 2. In Group 3 liver showed abnormal erythrocytes and electron dense granular material deposition (cadmium) whereas Group 4 showed multiple electron dense granular material deposition (lead and cadmium). Similar changes were noted [7, 10]. The changes recorded in Group 2, 3 and 4 was attributed to the toxic action of metals.

TEM section of Group 2 liver showed dilated sinusoids, swollen to condensed and pyknotic nucleus with electron dense chromatin material in nucleus. Cytoplasm of these cells showed vacuolation, granular cytoplasm and electron dense material in cytosol. Mitochondrial changes like swollen to condensed mitochondria, increased number of mitochondria and ruptured endoplasmic reticulum [10, 32, 19].

Group 3 rats liver showed loss of architecture and most of the hepatocytes showed eccentrically placed nucleus, collapsed nuclear membrane, pyknotic and rhexis of nuclei, clumping of chromatin material at one side. Cytoplasmic vacuolation, electron dense material in mitochondria and thickened

intercellular junction were also noticed [5, 7].

Liver of Group 4 rats revealed complete loss of architecture, shrunken cell and loose cell junctions. Condensed and eccentrically placed nucleus with nucleolus and condensed electron dense material in mitochondria were observed in addition to the changes mentioned above (Group 2 and Group 3)(31). These ultrastructural changes were also supported by biochemical and histopathological findings of the present study and possible reason for these changes might be due to the cytotoxicity caused by high production of free radicals (ROS and RNS) which was also supported by increased levels of TBARS and reduced GSH in liver.

The ultrastructure of Group 2 kidney section revealed loss of architecture, severe dilation of intertubular area and loss of tubular epithelium topography. Swollen nucleus with condensed nucleolus and margination of brush border were also observed in few sections. Cytoplasm showed vacuolation and swollen mitochondria with electron dense material in matrix [3].

Group 3 kidney of rats showed vacuolar degeneration and dilation of tubules. Some tubules showed degeneration of epithelial cells with loss of nucleus and swollen mitochondria. Epithelium of tubules showed dilation of nuclear pore along with margination of chromatin material. Other sections revealed disruption of nuclear membrane, pyknotic nuclei and electron dense round bodies in the nucleus, retention of brush border and condensed cytoplasm along with mitochondria.

Kidney of Group 4 rats showed complete loss of architectural details with only nucleus and mitochondria and other subcellular organelles were indistinct. Other sections revealed thick nuclear membrane, narrow and tight inter tubular junction, distorted chromatin, vacuolated cytoplasm and loss of nucleus. The perinuclear vesiculation and distorted mitochondria arranged in the form of rows around nucleus were observed. These ultrastructural changes were in agreement with other investigators [3, 6, 25, 30, 31]. These changes might be due to increased lipid peroxidation and increased ROS production due to heavy metal exposures which might interfere with mitochondrial sulphyhydral and thiol groups, leading to the permeability transition and cell death [29].

Conclusion

In conclusion, this study shows that lead and cadmium are the potent toxicant which can cause damage of tissue architecture and produce subcellular changes. Lead and cadmium administered in combination has a potentiated effect. It is also concluded that lead and cadmium are the potent inducers of oxidative damage of liver and kidney. The present study therefore provides investigatory evidence of supporting lead and cadmium toxicity in albino Wistar rats.

Acknowledgement

Authors are thankful to Associate Dean, College of Veterinary Science, Rajendranagar, Hyd. For providing necessary facility to carry out the investigation.

References

1. Al-Naimi RA, Abdulhadi D, Zahroon OS, Al-Taae EH. Toxicopathological study of lead acetate poisoning in growing rats and the protective effect of crystien or calicium. Al-Anbar. J Vet Sci. 2011; 4:26-39.
2. Alcaraz-Contreras Y, Mendoza-Lozano RP, Martínez-Alcaraz ER, Martínez-Alfaro M, Gallegos-Corona MA, Ramírez-Morales MA *et al*. Silymarin and dimercaptosuccinic acid ameliorate lead-induced nephrotoxicity and genotoxicity in rats. Hum Exp Toxicol. 2016; 35(4):398-403.
3. Anilkumar B, Gopala Reddy A, Anand Kumar A, Ambica G, Haritha C. Toxicopathological interaction of lead and cadmium and amelioration with N-Acetyl-L-Cysteine. Vet World. 2013; 6(10).
4. Bozzala JJ, Russel LD. Electron Microscopy Principles Techniques for Biologists, Jones and Barlett Publishers, Sudbury, Massachusetts. 2nd Edition. 1998, 19-45, 72-144.
5. Chang ES, Oh JS. Ultrastructural Changes of Lead Acetate Induced Liver Injury in Rats. Korean J Pathol. 1996; 30(3):184-198.
6. Deveci E, Söker S, Baran Ö, Tunik S, Ayaz E, Deveci S. Ultrastructural Changes in the Kidney Cortex of Rats Treated with Lead Acetate. Int J Morphol. 2011; 29(3):1058-106.
7. Faeder EJ, Chaney SQ, King LC, Hinners TA, Bruce R, Fowler BA. Biochemical and ultrastructural changes in livers of cadmium-treated rats. Toxicol App. Pharmacol. 1977; 39(3):473-487.
8. Gupta M. Ameliorative effect of cow urine in cadmium chloride induced toxicity In wistar rats (Doctoral dissertation, Chhattisgarh Kamdhenu Vishwavidyalaya, Durg), 2012.
9. Gurer H, Ercal N. Can antioxidants be beneficial in the treatment of lead poisoning? Free radic Biol Med. 2009; 29:927-945.
10. Hegazy AM, Fouad UA. Evaluation of Lead Hepatotoxicity; Histological, Histochemical and Ultrastructural Study. FMAR. 2014; 2(03):70.
11. Jarrar BM, Taib NT. Histological and histochemical alterations in the liver induced by lead chronic toxicity. Saudi J Biol Sci. 2012; 19(2):203-210.
12. Lemarie A, Lagadic-Gossmann D, Morzadec C, Allain N, Fardel O. Cadmium induces caspase-independent apoptosis in liver Hep3B cells: role for calcium in signaling oxidative stress-related impairment of mitochondria and relocation of endonuclease G and apoptosis-inducing factor. Free Radic Biol Med. 2004; 36:1517-1531.
13. Liu Y, Templeton DM. Initiation of caspase-independent death in mouse mesangial cells by Cd2+: involvement of p38 kinase and CaMK-II. J Cell Physiol. 2008; 217:307-318.
14. Luna GLHT. Manual of Histological and Special Staining Techniques, 2nd Edition. 1968; 1-5:9-34.
15. Nehru B, Kaushal S. Alterations in the hepatic enzymes following experimental lead poisoning. Biol Trace Elem Res. 1993; 38(1):27.
16. Oladipo OO, Ayo JO, Ambali SF, Mohammed B. Evaluation of hepatorenal impairments in Wistar rats co-exposed to low-dose lead, cadmium and manganese: insights into oxidative stress mechanism. Toxicol. Mech. Methods. 2016; 26(9):674-684.
17. Pandya CD, Pillai PP, Gupta SS. Lead and cadmium co-exposure mediated toxic insults on hepatic steroid metabolism and antioxidant system of adult male rats. Biol Trace Elem Res. 2010; 134(3):307-317.
18. Pandya C, Pillai P, Nampoothiri LP, Bhatt N, Gupta S. Effect of lead and cadmium co-exposure on testicular steroid metabolism and antioxidant system of adult male rats. Andrologia. 2012; 44(s1):813-822.
19. Park KK, Kim YH, Kwon KY, Chang ES, Chang MU.

Light Electron Microscopic Study in Rat Livers Following Cadmium Chloride Administration. Korean J Pathol. 1992; 26(1):28-39.
20. Piomelli S. Childhood lead poisoning. *Pediatr*. Clin. North Am. 2002; 49(6):1285-1304.
21. Prabu Milton S, Muthumani M, Shagirtha KK. Protective effect of Piper betle leaf extract against cadmium-induced oxidative stress and hepatic dysfunction in rats. Saudi. J Biol. Sci. 2012; 19(2):229-239.
22. Rani AU, Ramamurthi R. Histopathological alterations in the liver of freshwater teleost Tilapia mossambica in response to cadmium toxicity. Ecotoxicol Environ Saf, 1989; 17(2):221-226.
23. Renugadevi J, Prabu SM. Naringenin protects against cadmium-induced oxidative renal dysfunction in rats. Toxicology. 2009; 256(1):128-134.
24. Snedecor GW, Cochran WG. Statistical methods. Affiliated East West Press Pvt. Ltd., New Delhi, 13, 8th edn, 1994, 1467-1473.
25. Sujatha K, Srilatha CH, Anjaneyulu Y, Amaravathi P. Lead acetate induced nephrotoxicity in wistar albino rats, pathological, immunohistochemical and ultra structural studies. Int J Pharm Bio Sci. 2011; 2(2):B459-B469.
26. Suleman M, Khan AA, Hussain Z, Zia MA, Roomi S, Rashid F *et al*. Effect of lead acetate administered orally at different dosage levels in broiler chicks. AJEST. 2011; 5(12):1017-1026.
27. Suradkar SG, Vihol PD, Patel JH, Ghodasara DJ, Joshi BP, Prajapati KS. Patho-morphological changes in tissues of Wistar rats by exposure of Lead acetate. Vet World. 2010; 3(2):82-4.
28. Tarasub N, Tarasub C, Ayutthaya WDN. Protective role of curcumin on cadmium-induced nephrotoxicity in rats. JECE. 2011; 3(2):17-24.
29. Wang L, Li J, Li J, Liu Z. Effects of lead and/or cadmium on the oxidative damage of rat kidney cortex mitochondria. Biol Trace Elem Res. 2010; 137(1):69-78.
30. Wang L, Lin S, Li Z, Yang D, Wang Z. Protective effects of puerarin on experimental chronic lead nephrotoxicity in immature female rats. Hum Exp Toxicol. 2013; 32(2):172-185.
31. Yuan G, Dai S, Yin Z, Lu H, Jia R, Xu J *et al*. Toxicological assessment of combined lead and cadmium: acute and sub-chronic toxicity study in rats. Food Chem Toxicol. 2014; 65:260-268.
32. Zhang YM, Xue-Zhong LIU, Hao LU, Li MEI, Zong-Ping LIU. Lipid peroxidation and ultrastructural modifications in brain after perinatal exposure to lead and/or cadmium in rat pups. Biomed Environ Sci. 2009; 22(5):423-429.